Journal of Building Engineering 35 (2021) 102061

Contents lists available at ScienceDirect

Journal of Building Engineering

journal homepage: http://www.elsevier.com/locate/jobe

LCC-based framework for building envelope and structure co-design considering energy efficiency and natural hazard performance

Zhenglai Shen [a], Hongyu Zhou [a,*], Som Shrestha [b]

[a] Department of Civil and Environmental Engineering, University of Tennessee, Knoxville, TN, 37996, USA
[b] Energy and Transportation Science Division, Oak Ridge National Laboratory, Oak Ridge, TN, 37830, USA

ARTICLE INFO

Keywords:
Building envelope
Energy efficiency
Hazard resistance
Life-cycle cost

ABSTRACT

This paper presents a life-cycle cost (LCC) informed co-design framework for building structures and envelope systems, holistically considering the influences of energy and natural hazard performance. The proposed method is consisted of a two-stage design and decision-making process, aiming to provide a quantitative guideline for building's structural and envelope co-design based on the its geographic locations. First, the building's structural configuration and envelope type are selected based on the life cycle cost. Then, the long-term cost effectiveness of various energy-saving building envelope options (e.g., high-performance glazing and insulation) is evaluated to refine the envelope design. The proposed co-design framework was demonstrated through the case study of a medium-size office building archetype in three locations with distinct climate conditions and seismic activities (i.e., Los Angeles, Memphis, and Boston). The results highlighted the interplay between building's structural (seismic) performance and the cost-effectiveness of energy-saving design options – e.g., for buildings located in high-seismic regions, seismic enhancing designs greatly reduce the paybak period of high performance building envelope by reducing the seismic loss; whereas for buildings located in regions with cold climate and low seismic risk such as Boston, spatial frame with high insulation building envelope shows the lowest LCC.

1. Introduction

Buildings are responsible for 40% of primary energy consumption worldwide and 24% of greenhouse-gas emissions [1], significantly contributing to the causes of climate change. Meanwhile, building stocks are subjected to a wide range of climate-sensitive and site-specific hazards [2]. As the main physical assemblies that separate the conditioned building interior environment from the dynamic conditions of the exterior environment, approximately 39% of total primary building energy consumption can be attributed to heat transfer through building envelope [3]. Therefore, properly select and design building envelope has become a very important topic to ensure satisfactory requirements for building's performance on durability, energy efficiency, and sustainability. One common strategy to improve building's energy efficiency and reduce building's carbon footprint is through the use of high-performance envelope materials and assemblies such as vacuum insulated panels (VIPs) and vacuum insulated glass panels; however, high performance building envelopes are often associated with higher initial investment (i.e., materials to installation) as well as probable higher maintenance costs over time as compared to their traditional counterparts [4]. As a result, the adoption of new building envelope technologies needs to thoroughly account for their long-term cost effectiveness including various costs items from material purchasing, installation, maintenance, as well as potential repair and replacement over time.

Additional complications of this decision-making process arise as building envelope systems are frequently subjected to natural and manmade disastrous events such as wind storms, and earthquakes [5]. Under such circumstances, the building envelope component which features as part of nonstructural elements of the building likely experience various levels of damage that require repair or even total replacement, depending on the hazard resistance of building envelope components as well as the design of the structural backbone they are attached to Ref. [6]. A field reconnaissance following Hurricane Katrina conducted by Mosqueda et al. [7] shows that extensive losses were coming from nonstructural damage to claddings, windows, and roof-mounted equipments in addition to water damage in the interior of many buildings. In addition, the damage of envelope, especially façades, caused by earthquakes, is also well-documented in literature [8] and it contributes largely to the overall building losses. From an economic

* Corresponding author. 851 Neyland Drive, 417 John D. Tickle Building, Knoxville, TN, 37996-2313, USA.
E-mail address: hzhou8@utk.edu (H. Zhou).

https://doi.org/10.1016/j.jobe.2020.102061
Received 25 August 2020; Received in revised form 21 November 2020; Accepted 1 December 2020
Available online 3 December 2020

standpoint, higher performance building envelope options, although more energy-efficient and cost-saving during building operation, may be adversely affected by the potential loss caused by natural hazard events.

Life-cycle cost (LCC) analysis has been used to evaluate the cost and benefit of high-performance building envelopes for both commercial and residential buildings [9–12]. Kneifel [9] analyzed the energy performance of 12 prototypical commercial buildings in 16 US cities, and the results show that energy efficiency envelope options (i.e., high-performance glazing and increased envelope insulation) lead to the decrease of energy use in new commercial buildings by 20–30% on average, and a reduction of LCC about 3.5% in 10 year service life. Mahlia and Iqbal [10] demonstrated through LCC analysis that increasing wall insulation can lead to an energy saving of 65–77% in Maldives. Similar LCC analysis was carried out by Morrissey and Horne [11] to highlight the benefit of high energy efficiency envelope for residential buildings in Melbourne, Australia. In addition, LCC analysis also was applied to evaluate the cost and benefit for green and living wall systems [12]. Most existing LCC analysis performed on building envelope systems only accounts for its initial cost, thermal performance (energy cost), and environmental impacts, with the assumption that the building envelope system will remain intact during the building's expected life cycle aside from regular maintenance [13]. However, building envelope components may experience damage due to the exposure to natural hazards depending on the geographic location where the building is situated in. For certain natural hazard event such as an earthquake, building's structural layout and design of buildings are expected to have influence on the hazard performance of building envelope since the damage level of nonstructural building elements are mostly dictated by the structural responses (e.g., interstory drift ratio or peak floor acceleration) [14]. The impact of building's structural performance when subjected to natural hazards on the loss and cost-effectiveness of nonstructural components (i.e., building envelope) calls for a more comprehensive method for evaluating the cost benefit of high-performance building envelope options. An earlier study conducted by Liu and Mi [13] developed a LCC-based decision making method to consider the potential loss caused by earthquake. Noshadravan et al. [15] performed a LCC analysis of residential buildings considering natural hazard risks, i.e., earthquake and hurricane. However, these studies did not consider the interaction between structural systems and the envelope options.

Researches also have been carried out to explore building's structural design and its impacts to economic and environmental cost with or without seismic risk [16–18]. Ji et al. [16] compared three decision-making methods that consider both cost and CO_2 emission in building structural design. Nadoushani and Akbarnezhad [17] studied the influence of structural system on the life cycle carbon footprint of buildings. Another research carried out by Belleri and Marini [18] studied the effects of seismic risk to environment in existing buildings of Italy by using the Pacific Earthquake Engineering Research (PEER) performance-based earthquake engineering (PBEE) framework. Although the aforementioned researches revealed the inherent impacts of building's structural design on its economic and environmental cost, they did not consider the interplay between structural system and other non-structural components (e.g., building envelop) and its implication on building's long-term energy efficiency.

In this research, a two-stage, LCC-informed decision-making process is developed for the co-design of building's structural and envelope systems, aiming to find the design combination that yield the lowest operational energy use and long-term life cycle costs. To achieve this objective, life-cycle cost assessment is used to quantify the costs associated with each offstage of building construction and operation, including the operational energy use and natural hazard resistance. The design inputs include building structural configuration, building envelope type, and envelope material options such as insulation and glazing. To illustrate the method developed herein, case studies are carried out on medium size office building archetypes located in three locations with distinct climate conditions and earthquake hazard exposures– i.e., Los Angeles, California (Mediterranean climate with high seismic activity), Memphis, Tennessee (mild climate with medium seismic activity) and Boston, Massachusetts (cold climate with low seismic activity), where the interaction between building's energy and hazard performances as impacted by the design selections are highlighted.

2. A two-stage LCC-informed decision-making process for energy efficient building envelope selection

Fig. 1 presents the two-stage LCC-informed building design decision-making process, which aims to provide a quantitative guideline for the co-design of building's structural and envelope systems based on the building's geographic location, as well as the associated climate condition and natural hazard exposures. In the first stage, a co-design of building's structural configuration and the envelope type is conducted based on the life-cycle cost (LCC) analysis, where the initial construction cost and the present value of cumulative future costs including building maintenance, energy consumption, greenhouse gas (GHG) emissions, and the expected repair and replacement costs caused by natural hazard events (e.g., earthquake) are considered. The initial design is based on the long-term cost effectiveness of design options with the consideration of the impacts of the building structural hazard resistance on the damage fragility of structural and nonstructural components including building's envelope elements. Once the preliminary design is completed, discounted payback period (DPP) analysis is carried out in the next step to refine energy-saving features such as high-performance window glazing (e.g., low-E, vacuum insulated, thermochroic glazing) and high-performance insulation (e.g., vacuum insulated panels) etc. The new design approach allows for a holistic consideration of building's hazard resilience, energy efficiency, and long-term cost effectiveness in building design, which will improve the decision-making process for selecting building design alternatives, retrofit and/or insurance strategies. The integrated consideration of multiple facets of building's performance during the design phase may also bring improvements to building codes and green rating systems.

2.1. Life-cycle cost analysis considering both energy efficiency and hazard resistance

2.1.1. Life-cycle cost

Life-cycle cost (LCC) is the discounted value of the sum of costs and benefits that occur at the end of the building service life, T_l, considered. If all attributes and consequences of a decision concerning a building can be expressed in monetary terms then an optimal decision will be the one that minimizes the LCC. For a building, the LCC may include initial construction cost, maintenance cost, operational energy cost, and the repair/replacement costs due to exposure to natural hazard. The expected LCC up to T_l may be calculated as:

$$LCC(T_l) = C_C + C_M(T_l) + C_E(T_l) + C_S(T_l) \tag{1}$$

where C_C is the initial construction cost (includes materials and labor), $C_M(T_l)$, $C_E(T_l)$, and $C_S(T_l)$ are the net present values (NPVs) of future maintenance cost, operational energy cost, and expected seismic monetary loss at the end of the period of service life, T_l, respectively. The NPV terms, $C_i(T_\tau)$, is calculated as:

$$C_i(T_\tau) = \sum_{j=1}^{T_\tau} \left(\frac{1}{1+\alpha}\right)^j C_i^{annual} \tag{2}$$

where, C_i represents cost items (i.e., maintenance cost) and C_i^{annual} are their corresponding annual values, and α is the annual discount rate. Note that Equation (2) only considers the time value of money, whilst other factors such as demand and requirement are not considered. For operational energy cost, a projected price index is used to adjust the

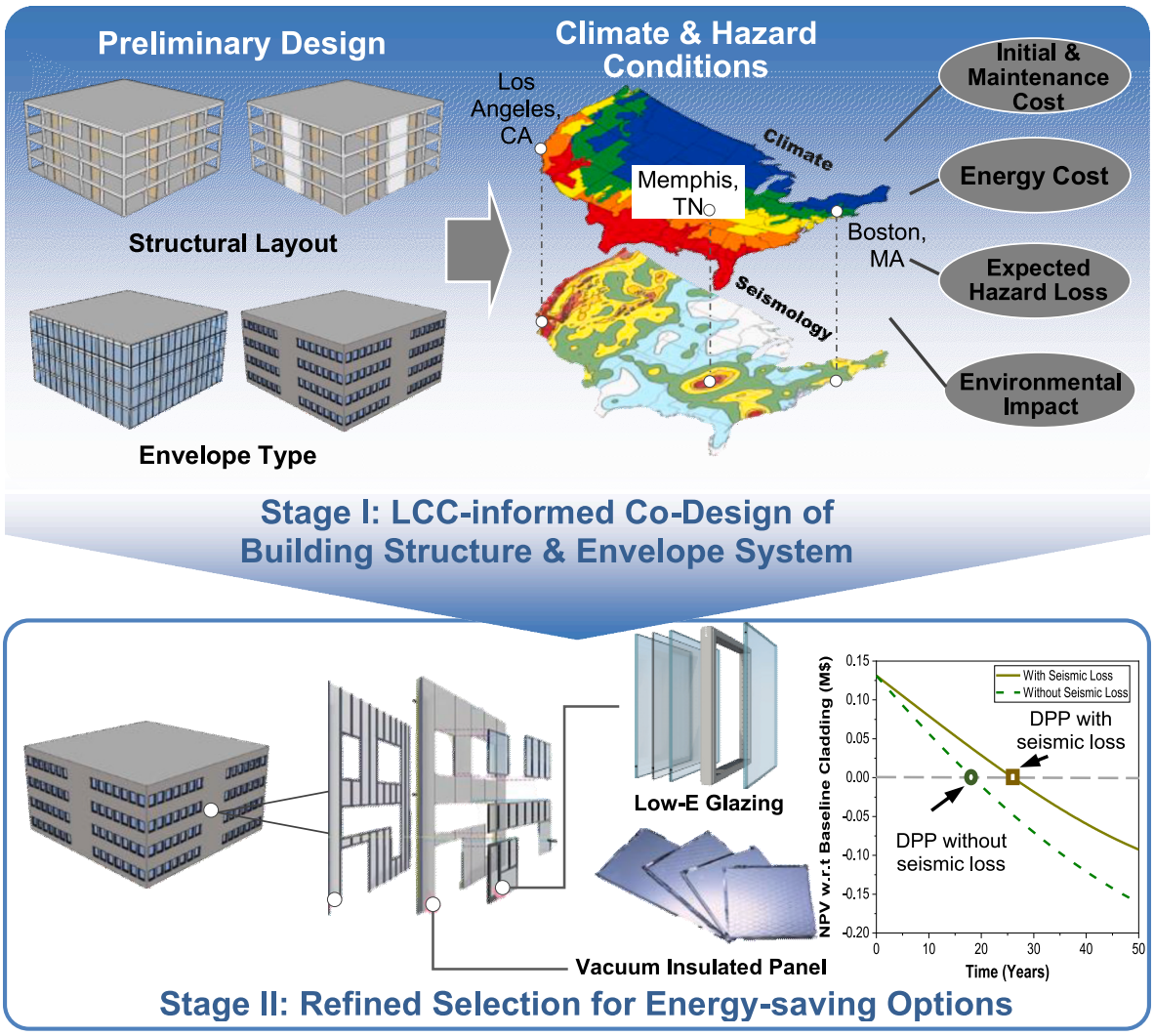

Fig. 1. A two-stage LCC-informed decision-making process for building structure and envelope design.

future unit energy price (e.g., electricity) based on NIST Handbook 135 [19] and the projected price index is extrapolated to the future 50 years - i.e., the projected price index calculated by the Office of Management and Budget (OMB) Circular A-94 method is used, where −0.3% and 0.6% discount rates are assumed for short term (1–10 years) and long term (11–30 years) to reflect the difference between expected inflation and nominal interest rate. The long term projected price (i.e., 11–30 years) is extrapolated to the end of the life-cycle, i.e., 50 years.

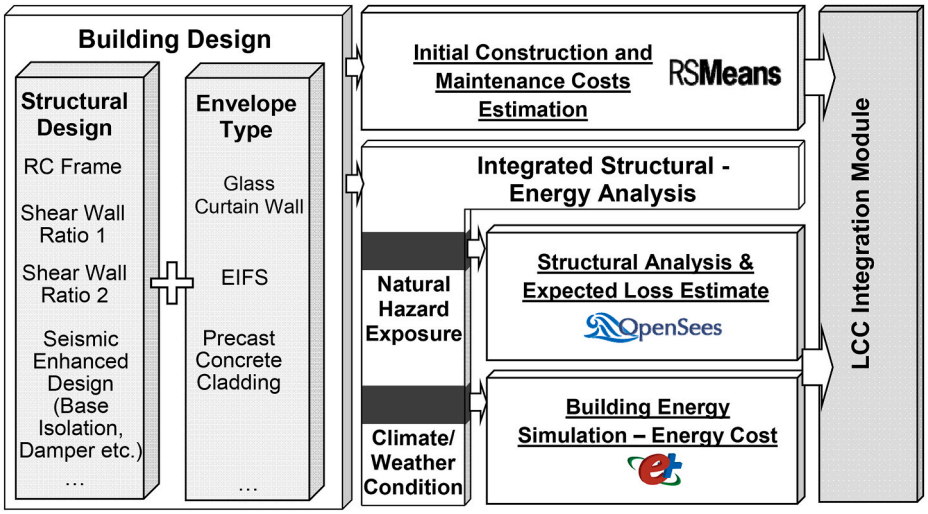

Fig. 2. The analysis modules employed by this study to obtain the LCC index to support preliminary building design.

For the initial design stage (*Stage I*), the LCC of archetype buildings with various structural configurations and envelope types are assessed following the analysis procedure as shown in Fig. 2. The initial construction was estimated using RSMeans [20] and maintenance cost was estimated using the Whitestone M&R data [21] and adjusted using the city-based cost index. The annual energy consumption is obtained using whole-building energy simulation and the annual energy costis then calculated based on local energy prices.

2.1.2. Estimate economic loss due to seismic hazard

The seismic loss is estimated following the PEER's performance-based earthquake engineering (PBEE) procedure [22] as outlined in Fig. 3. First, the site hazard is quantified through a hazard model. For the seismic hazard considered in this study, the rate of exceedance of seismic hazard is normally expressed as a function of the seismic intensity measure (*IM*) – e.g., peak ground acceleration (PGA) or response spectrum acceleration (S_a)) [23]:

$$\lambda(IM>x)=\sum_{k=1}^{n_{source}}\lambda(IM_k>im_{\min})\int_{im_{\min}}^{im_{\max}}\times\int_0^{r_{\max}}P(IM>x|im,r)f_{IM_i}(im)f_{R_i}(r)drdim \tag{3}$$

where n_{source} is the number of seismic source considered; $\lambda(IM>x)$ is the mean annual frequency of exceedance (MAFE) of $IM>x$; $\lambda(IM_k>im_{\min})$ is the rate of occurrence of earthquakes greater than $im_{\min}$ from the k-th earthquake source; $P(IM>x|im,r)$ is obtained from the ground motion attenuation law; $f_{IM_k}(im)$ and $f_{R_k}(r)$ are the probabilistic density functions (PDFs) for earthquake magnitude and distance.

For a given MAFE, the probability of exceeding a given ground motion intensity within a given time, t, is [22]:

$$P(IM)=1-e^{-\lambda(IM)t} \tag{4}$$

Thus, the probability of each IM level is obtained from Equation (4) through:

$$p(IM_m)=\begin{cases}P(IM_m) & \text{if } m=\#\text{ of } IM \text{ levels}\\ P(IM_m)-P(IM_{m+1}) & \text{otherwise}\end{cases} \tag{5}$$

Then, structural analysis is performed to obtain the response of a structure to different levels of earthquake hazard. For each intensity level, the structural responses in terms of selected engineering demand parameters (EDPs) – e.g., interstory drift ratio (IDR)), are computed from nonlinear time history analyses. For EDP_ξ with a given hazard intensity measure, IM_m, its probability may follow the lognormal distribution with the cumulative distribution function (CDF) expressed as:

$$P(EDP_\xi\le edp_\xi|im_m)=\Phi\left(\frac{\ln(edp_\xi|im_m)-\ln\mu_\xi}{\beta_\xi}\right) \tag{6}$$

where μ and β are the median and logarithmic standard deviation of edp_ξ, respectively.

Thus, the probability of a damageable building component (structural or non-structural), n, reaching certain damage measure, $DM_{n\eta}$, is defined by a fragility function [22]:

$$p(DM_{n\eta}|EDP_\xi)=\begin{cases}P(DM_{n\eta}|EDP_\xi) & \text{if } \eta=\#\text{ of } DM \text{ states}\\ P(DM_{n\eta}|EDP_\xi)-P(DM_{n(\eta+1)}|EDP_\xi) & \text{otherwise}\end{cases} \tag{7}$$

Lastly, a loss model is defined to quantify the probability distribution of monetary loss (due to repair and replacement) for a building element reaching given damage level, $P(L_{n\varsigma}|DM_{n\eta})$. The expected annual seismic monetary loss of a building is obtained by Refs. [22]:

$$C_S^{annual}=\lambda\sum_n\sum_\eta\sum_\xi\sum_m L_{n\varsigma}P(L_{n\varsigma}|DM_{n\eta})p(DM_{n\eta}|EDP_\xi)p(EDP_\xi|IM_m)p(IM_m) \tag{8}$$

2.1.3. Fragility model of building envelope component

For the component-level loss estimation, FEMA P-58 PACT [6] was used to obtain fragility parameters, repair cost/time, casualty and fatality consequence function for the structural and non-structural components. The probability distribution of damage state for a building element, i.e., the component fragility function, is assumed to follow a lognormal distribution function of the engineering demand parameters, as expressed by Equation (6). For the building envelope systems considered in this study – i.e., glass curtain wall (GCW), exterior insulation finishing system (EIFS), and precast concrete cladding (PCC), the parameters of Equation (6) as well as the repair costs for each damage state are enlisted in Tables 1–3. The repair cost at a specific damage state is estimated as a function of the replacement cost of the corresponding component based on the method outlined in FEMA P-58 [6]. The replacement cost is estimated as 1.5 folds of the construction costs, while the potential cost differences caused by different floor levels (scaffolding etc.) are neglected for simplicity.

For the stick-built GCW cladding system, the damage state (*DS*) is defined as a function of the interstory drift ratio since the damage is mainly caused by the lateral-displacement induced deformations [24]. Table 1 lists the damage states and the corresponding repair costs of GCW claddings for the baseline double-pane glazing (DPG) and three other high-performance glazing options – i.e., the triple-glazed low-E glass (TriLE), the vacuum glazing (VacG), and the thermochromic glazing (TCG). At DS1, the gasket seal starts to fail which can be repaired

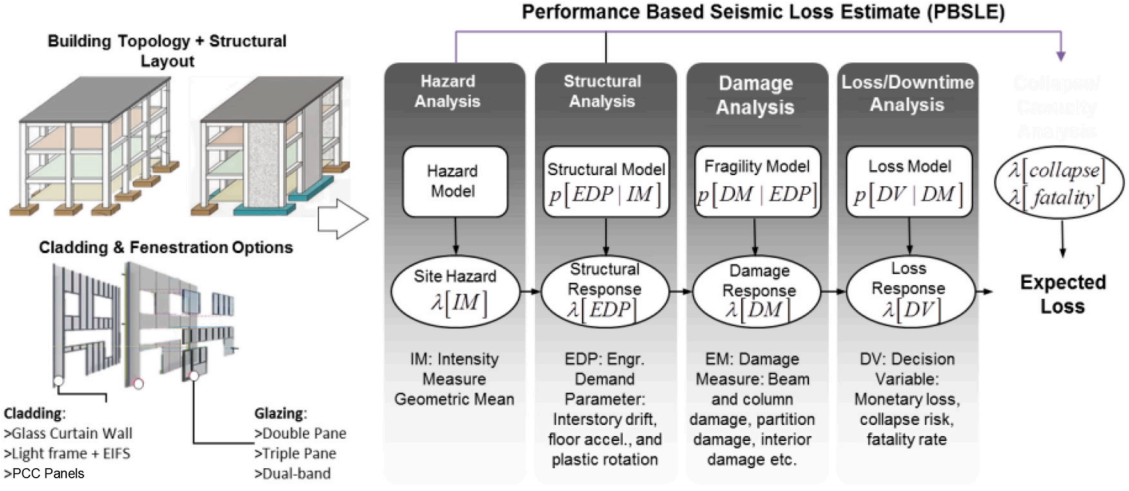

Fig. 3. Schematic of performance-based earthquake engineering methodology [22].

Table 1
Damage states and repair costs of GCW cladding.

Damage State	Description	μ	β	Item repair cost	Repair cost ($/m^2) (DPG/TriLE/VacG&TCG[a])
DS1	Remove glass panel and replace damaged gaskets	0.026	0.25	0.5 × replacement cost	304/392/473
DS2	Replace cracked glass panel	0.0268	0.25	0.8 × replacement cost	486/627/757
DS3	Replace cracked glass panel; cover exposure in meantime	0.0339	0.25	replacement cost	607/785/946

[a] VacG and TCG are assumed to have the same construction and repair costs.

Table 2
Damage states (DS) and repair costs of EIFS cladding.

Damage State	Description	μ	β	Item repair cost	Repair cost ($/m^2) EPS-DPG/MAI-DPG/MAI-TriLE/VIP-TriLE
DS1	Screws pop-out, minor cracking of EIFS panels	0.0021	0.6	0.2 × replacement cost of EIFS panel	56/63/63/80
DS2	Initial cracking of caulking	0.0048	0.15	0.25 × replacement cost of caulking	61/68/68/85
DS3	Glass pane contact and small cracking at perimeter	0.006	0.12	0.2 × replacement cost of window glazing	95/102/116/133
DS4	Moderate cracking or crushing of EIFS panels	0.0071	0.45	0.4 × replacement cost of EIFS panel	151/165/179/214
DS5	Failure of caulking	0.0088	0.25	replacement cost of caulking	166/180/194/229
DS6	Glass translation and gasket pull-out	0.011	0.2	0.5 × replacement cost of window glazing	217/231/266/301
DS7	Significant cracking and buckling of studs and tearing of tracks	0.012	0.45	replacement cost of EIFS panel	385/421/456/542
DS8	Observable cracking in glass	0.016	0.19	0.8 × replacement cost of window glazing	436/472/528/614
DS9	Major cracking and glass fallout	0.020	0.16	replacement cost of window glazing	470/506/576/662

by replacing damaged gaskets; at DS2, replacing cracked glass panels maybe required; lastly, at DS3 total replacement of the façade is required.

An exterior insulation finishing system (EIFS) cladding is normally comprised of EIFS panels and window fenestrations attached to the cold-formed steel framing. The damage states of EIFS are mostly attributed to the damages of silica caulking, the EIFS panel, windows (both frame and glazing), fasteners, and the supporting cold-formed steel framing. Table 2 lists the damage states and corresponding repair costs of the EIFS cladding with different insulation and glazing options – i.e., three insulation options: the R-13 EPS baseline, the vacuum insulated panels with fumed silica core (VIP), and the modified atmosphere insulation (MAI) recently developed by Oak Ridge National Laboratory [25], in conjunction with two glazing options: the double-pane glazing (DPG) and triple-glazed low-E glass (TriLE). The damage of EIFS system starts with minor cracking of the EIFS panels and caulking, followed by window glazing damage, crushing of EIFS panels and buckling of the cold-formed steel framing members, and finally glass fallout, where the damage state definitions for caulking, window glazing, and EIFS panel are adopted from Refs. [6,26,27], respectively.

Table 3
Damage states and repair costs of PCC Cladding [26,28].

Damage State	Description	μ	β	Item repair cost	Repair cost ($/m^2)
DS1	Initial cracking of caulking	0.0048	0.15	0.25 × replacement cost of caulking	5
DS2	Onset of yielding of threaded rod	0.0079	0.25	0.3 × replacement cost of push-pull connector	48
DS3	Failure of caulking	0.0088	0.25	replacement cost of caulking	60
DS4	Significant yielding of thread rod	0.014	0.25	0.6 × replacement cost of push-pull connector	104
DS5	Hair-like cracks of PCC panel	0.0192	0.20	Cosmetic repair with 13.2$/m^2	117
DS6	Fracture of thread rod	0.025	0.25	replacement cost of push-pull connector	175
DS7	Surface cracks and corner crushing of PCC panel	0.0339	0.20	Epoxy injection and concrete patching with 137.4$/m^2	299

There are typically three types of Pre-cast concrete (PCC) claddings: (1) type C1 cladding consists spandrel panels with glazing between stories; (2) type C2 cladding consists of spandrel panels that span the full height of the story with windows inside the spandrel panels; and (3) type C3 cladding is similar to type C1 with column cover panels spanning between floors. The type C2 cladding is selected in this study since the windows are protected from seismic damage and presents the least seismic loss of all three types of PCC claddings [26]. The PCC panels are normally attached to the building's structural frame through push-pull connections (threaded rods) and vertical bearing connections, see Fig. 4. Due to the rigidity of C2 panels, window glazing may experience little to no damage under low intensity earthquakes, whereas most damages occurs in the connectors [26,28]. At higher displacement level, the damage on PCC panels are normally consisted of cracks or corner crushing caused by pounding of adjacent panels [28]. Table 3 summarizes the damage states of the PCC cladding and the corresponding repair cost for each DS level. The definition of damage states are adopted from the studies conducted by McMullin and Nguyen [29], Hunt [26] and Baird [28]. The damage of PCC cladding starts with cracking of the silica caulking, followed by yielding of thread rod of push-pull connector and failure of the silica caulking. As the interstory drift ratio increases, significant yielding of thread rod and hair-like cracks of PCC panel occurs. Lastly, thread rod starts to fracture, and PCC panel exhibits surface cracks and corner crushing.

2.2. Discounted payback period analysis for energy saving design options

The discounted payback period (DPP) analysis is used to determine the cost-effectiveness of an enhanced design option. DPP analysis gives the number of years it takes to break even from undertaking the initial investment by discounting future benefits and recognizing the time

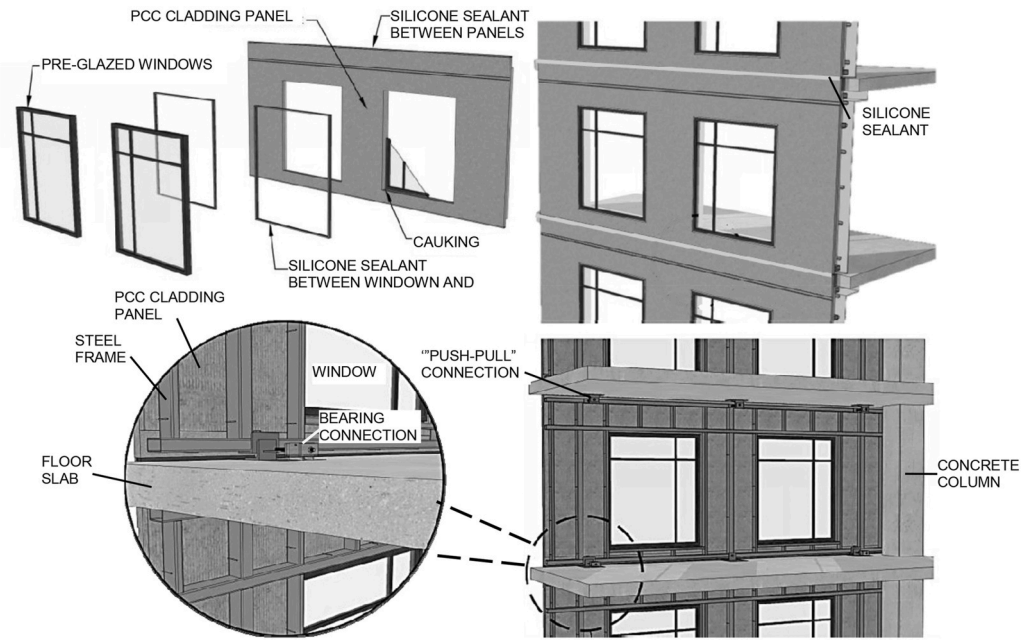

Fig. 4. PCC cladding configuration and detailings

value of money. The DPP of the energy-saving design options considered in this study are obtained through solving:

$$\left(C_C^{HP} + \sum C_i^{HP}(T_{DPP})\right) - \left(C_C^{BL} + \sum C_i^{BL}(T_{DPP})\right) = 0 \tag{9}$$

where the superscripts *HP* and *BL* represents high-performance alternative and the baseline, respectively; $\sum C_i^{HP}(T_{DPP})$ and $\sum C_i^{BL}(T_{DPP})$ are the net present values (NPVs) of the energy-saving design options (i.e., high-performance insulations and glazing) and their corresponding ASHREA 90.1 complied baseline, respectively.

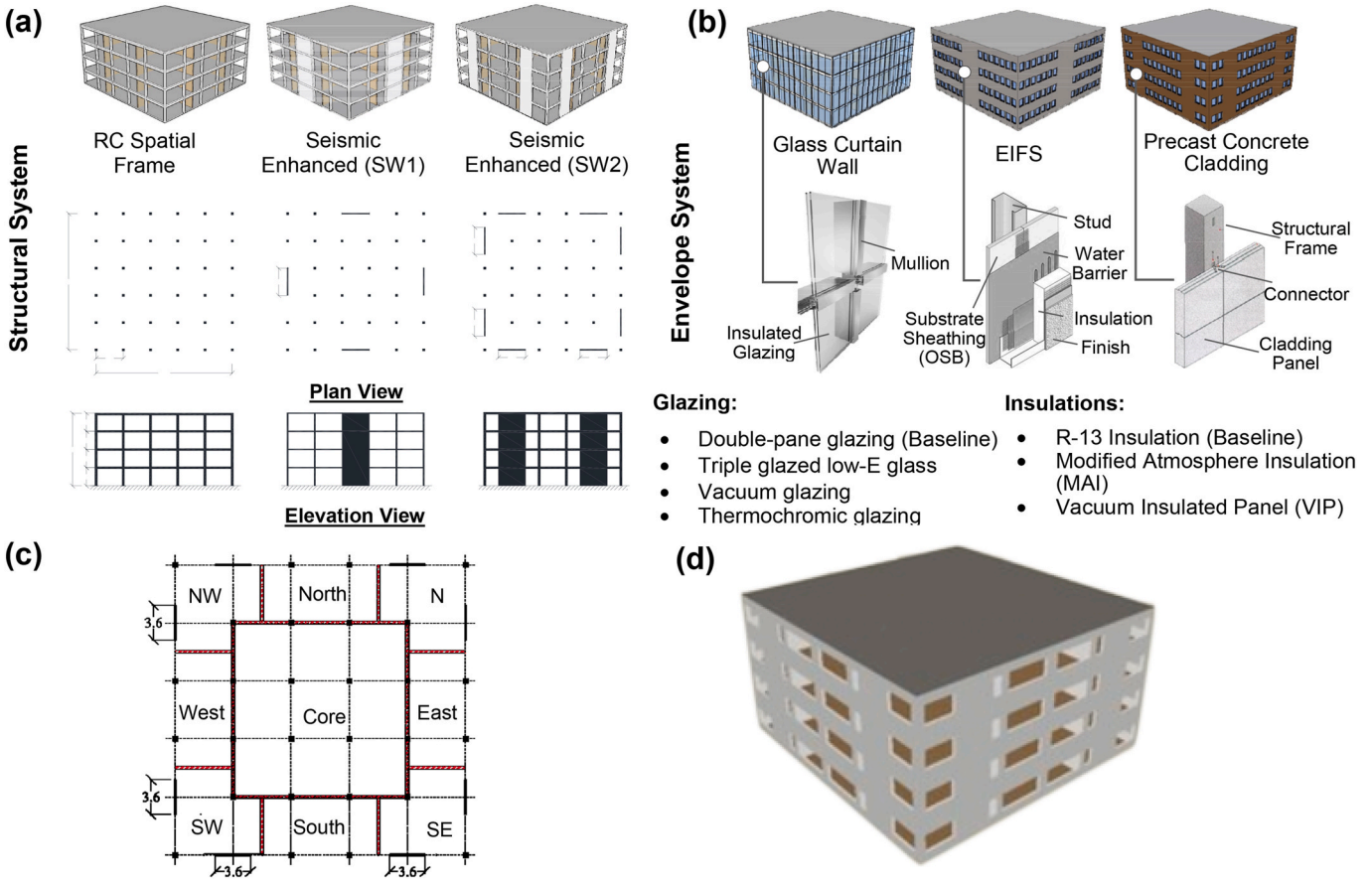

Fig. 5. The (a) floor plans; (b) envelope types; and (c) thermal zones of building archetypes; and (d) EnergyPlus model.

3. Case study with archetype buildings

3.1. Archetype configurations

To demonstrate the LCC-informed co-design framework, a four story reinforced concrete (RC) office building archetype is designed in three geographic locations – i.e., Los Angeles (CA), Memphis (TN), and Boston (MA). The building is 30 m × 30 m with column span of 6 m and story height of 4 m. The building archetype is adopted from AlHamaydeh et al. [30] to represent typical medium size office buildings. For each location, three structural configurations were considered, namely the spatial frame (SF), shear wall layout 1 (SW1), and shear wall layout 2 (SW2), as illustrated in Fig. 5 (a). The shear wall designs represent the seismic enhanced design options – SW1 has only one shear wall at the middle of each perimeter of the building (6 m length), while SW2 has two 3.6 m shear walls on each side of the perimeter. SW1 and SW2 represent different shear wall layouts and shear wall to floor area ratios. The structural design was performed according to the specifications of ACI 318-14 and ASCE7-16, and the details can be found in Ref. [31].

Three building envelope types – i.e., the glass curtain wall (GCW), exterior insulation and finishing system (EIFS), and pre-cast concrete (PCC) cladding, are compared in this study due to their widespread use in commercial buildings. Fig. 5 (b) shows the schematics of each building envelope type. The envelopes are designed to meet ASHRAE 90.1 specifications [32] for climate zones 3B (Los Angeles, CA), 3A (Memphis, TN), and 5A (Boston, MA).

For GCW, four types of glazing materials – i.e., the double pane glass (DPG) is used as the baseline, and triple pane low-E glazing (TriLE), vacuum insulated glazing (VacG), and thermochromic glazing (TCG) are studied as the high-performance energy-saving design alternatives. The solar thermal properties of each glazing option and their costs (for Los Angeles, CA) are listed in Table 4. The cost of glazing used for GCW and that for EIFS/PCC (windows) are different due to the different framing structure and installation processes. The mid-rise stick system is assumed for GCW, which requires vertical mullions to be installed and anchored to the floor slabs and additional components including horizontal mullions and spandrel panels are attached once the vertical mullions are in place; whereas the glazing of EIFS/PCC cladding typically requires lower labor costs as compared to the GCW system.

For the EIFS and PCC, the designed U-values, layup, and costs are listed in Table 5. The claddings are named by the insulation and glazing type – e.g., 'EIFS-EPS-DPG' represents EIFS cladding system with the baseline R-13 EPS insulation and double-pane glazing as window glazing. It is noted that, the PCC claddings are considered as a mass wall system, which can adopt higher U-values in design [32]. The cost listed in Table 5 is based on the prices in Los Angeles, CA, and city-based construction cost index [20] is applied to adjust the construction costs of the envelope systems for the studied regions, see Table 6.

3.2. Building energy simulation

To quantify the energy consumption and costs during the building's operational phase, the whole-building energy consumption analysis is conducted using EnergyPlus. For each floor, the archetype buildings are divided into nine thermal zones with an 18 m × 18 m core area at the center and eight boundary zones on the perimeter of the archetype buildings, see Fig. 5 (c). For the EIFS and PCC claddings, a window to wall ratio (WWR) of 37.5% was used. The model settings and schedules, such as occupancy and lighting, offcie equipments, ventilation, air condition heating and cooling, are adopted from the medium office building archetype published by the US Department of Energy [35]. The building has an occupancy of 18.58 m^2/person. The lighting intensity and internal heat gain from office equipments are 10.76 and 8.08 W/m^2 respectively. The variable air volume (VAV) reheat HVAC system is used with electricity for cooling and natural gas for heating [32]. The VAV reheat HVAC system has been applied to about 65% of medium office buildings in US according to the 2013 report of Zhang and Liu [36]. The set points for heating and cooling are 21.1 °C and 23.9 °C, respectively, with setback temperature of 15.6 °C for heating and 29.4 °C for cooling, respectively.

3.3. Structural analysis under seismic hazard

The building structures were designed using SAP2000 and modeled using OpenSees for nonlinear seismic analysis. Fiber elements were used to model the RC beams and columns, and SFI-MVLEM elements were

Table 4
Solar thermal properties and costs of glazing materials.

Glazing Type	SHGC	Direct solar transmition	Visible Light transmission	U-value	Cost (GCW/Window)
	(–)	(–)	(–)	(W/m^2K)	($/$m^2$)
DPG (Baseline)	0.25	0.21	0.31	2.58	405/306
TriLE	0.22	0.13	0.27	1.20	523/424
VacG	0.25	0.29	0.58	0.80	631/532
TCG*	0.10	–	–	1.07	631/532

*Solar heat gain coefficient (SHGC) and U-value calculated in Window 7.7 under the environmental condition of NFRC 100-2010.
*The costs of DPG, TriLE, and VacG and TCG are adopted from RS Means [20], BEopt [33], and [34], respectively.

Table 5
Designed exterior walls/claddings and costs.

Cladding	U-value	Layup information	Heat capacity	Cost[a]
	(W/m^2K)	(cm)	(kJ/m^2K)	($/$m^2$)
EIFS-EPS-xxx	0.442	Stucco/EPS/PB (2.5/7.6/1.2)	51	298
EIFS-MAI-xxx	0.230	Stucco/MAI/PB (2.5/5.1/1.2)	50	336
EIFS-VIP-xxx	0.155	Stucco/VIP/PB (2.5/5.1/1.2)	50	431
PCC-EPS-xxx	0.590	Stucco/C/EPS/C/PB (2.5/5/5.1/15/1.2)	454	506
PCC-MAI-xxx	0.223	Stucco/C/MAI/C/PB (2.5/5/5.1/15/1.2)	454	551
PCC-VIP-xxx	0.151	Stucco/C/VIP/C/PB (2.5/5/5.1/15/1.2)	454	646

PB = plasterboard, C = concrete.
[a] Cost is estimated by RSMeans™

Table 6
City-based cost index and energy prices of Los Angeles, Memphis, and Boston.

City	Construction cost index	City-based cost index	Electricity price	Natural gas price
	(–)	(–)	($/kWh)	($/therm[a])
Los Angeles	1.123	0.985	0.181	1.238
Memphis	0.861	0.860	0.107	0.653
Boston	1.139	1.056	0.218	1.331

[a] 1 therm = 29.3 kW h

used to model RC shear walls [37]. Due to their low self-weight, the influence of GCW and EIFS claddings on the dynamic responses of the archetype buildings are ignored, whereas the self-weight of PCC cladding is added as uniform distributed dead loads on the perimeter frame of archetype building. The first-mode periods of the archetype buildings are listed in Table 7.

For the collapse fragility analysis, 22 far-field ground motions are used per the recommendation of FEMA P-695 [38]. Incremental Dynamic Analysis (IDA) is used to evaluate collapse capacity of the archetypes. Then, the collapse capacity obtained from IDA is used to find the empirical CDF of the collapse fragility functions, and maximum likelihood method is used to fit a lognormal distribution function over the empirical CDF. Table 7 summarizes the expected collapse capacity, μ, and its corresponding logarithmic dispersion, β.

After the collapse fragility function of each archetype building is obtained, nonlinear time-history analysis is performed to obtain its structural responses (EDPs such as interstory drift ratios and peak floor accelerations) under the excitations of scaled ground motions [6]. Then, the obtained collapse fragility function along with the structural responses obtained from nonlinear structural time-history analysis are used as input to conduct seismic loss estimation using FEMA P-58 PACT [6].

4. Results and discussions

4.1. Co-design of structural and envelope systems based on LCC

4.1.1. Construction cost

Fig. 6 presents the construction costs of various structural systems and claddings. Generally, higher seismic demands lead to larger structural components size and higher construction costs. The construction costs of shear wall buildings, i.e., SW1 and SW2, are higher than their spatial frame (SF) counterparts due to the higher costs of substructure and additional costs of shear walls, see Fig. 6 (a). The construction cost of envelope depends on the cladding type, insulation materials, and glazing materials, see Fig. 6 (b). GCW cladding has a higher construction cost due to the high unit glazing cost and installation fee, see Table 4. EIFS cladding has a relatively lower cost as compared to PCC due to its lightweight feature with reduced material cost and installation labor cost. For GCW system the current market cost for double-pane glazing is ~260 $/m^2 [20], whereas it costs 380$/m^2 for triple-pane low-E glass [33] and 490 $/m^2 for vacuum glazing [34], thermochromic glazing has similar cost as that of vacuum glazing. Since materials are roughly 60–70% of the construction, the difference in glazing materials has led to 30–60% increase in overall construction cost of the envelope system. For EIFS, the cost for R-13 EPS insulation is 23 $/m2, while the costs for R-25 MAI and R-35 VIP are 60 $/m2 [25], and 155 $/m2 [39] respectively. For EIFS with R-13 EPS, the cost of insulation material is about 10%, while the costs of other components of EIFS cladding, i.e., substrate, adhesive between substrate and insulation, reinforcing mesh, finish coating and the install labor cost account about the remaining 90% of the construction cost. Adopting high-performance insulations, i.e., MAI and VIP, will increase about 13% and 44% of the overall construction cost. Adding high-performance glass to windows in an EIFS system typically will increase the construction cost by 20%. As for PCC, similar construction cost increase trend was observed as that for EIFS when adopting high-performance insulation material and high-performance glazing. However, the construction cost of PCC panel is higher than EIFS counterparts with an increasing of about 200 $/m^2. It is worthwhile to mention that the exterior of shear wall is not covered by the corresponding cladding because shear wall blocks the outdoor environment (see Fig. 5 for the layout of the cladding). Instead, a layer of insulation which compatible with the assigned cladding insulation material and stucco are used and therefore the cladding costs of shear wall (SW1 and SW2) buildings are lower than the spatial frame (SF) building.

Table 7
The first-mode periods and collapse fragility parameters of archetype buildings.

Buildings	GCW/EIFS			PCC		
	First-mode period	μ	β	First-mode period	μ	
	(sec)	(–)	(–)	(sec)	(–)	(–)
LA-SF	0.76	2.98	0.51	0.83	2.63	0.49
LA-SW1	0.27	4.18	0.39	0.29	4.03	0.44
LA-SW2	0.32	4.13	0.36	0.34	3.96	0.36
MP-SF	1.09	1.51	0.50	1.20	1.29	0.65
MP-SW1	0.35	2.26	0.37	0.37	2.17	0.38
MP-SW2	0.49	2.20	0.36	0.53	2.12	0.31
BS-SF	1.27	0.97	0.83	1.40	0.78	0.86
BS-SW1	0.45	1.34	0.81	0.48	1.30	0.75
BS-SW2	0.59	1.33	0.58	0.63	1.30	0.55

4.1.2. Maintenance cost

The maintenance cost is estimated by the Whitestone M&R data [21]. Two service lives (i.e., 30 years and 50 years) are considered for glazing materials – at the end of its service life, windows and glaszings will be replaced. Except for the scheduled minor repair of GCW at every five years and repair operable window of EIFS and PCC at every 15 years, an annual glazing cleaning fee of 1 $/m^2 is assumed to maintain the aesthetics of glazing. PCC panel typically has a service life of over 75 years and requires very little maintenance over the life span of the building. Its maintenance includes only occasional cleaning as aesthetically desired, and maintenance of the caulking and waterproofing systems. Therefore, a maintenance fee of 1 $/m^2 at every five years is assumed. On the other hand, EIFS panel may be subject to moisture damage, caulking failure and inability to drain, and thus needs more maintenance efforts. For this study, the annual inspection and minor repair costs of 0.5 $/m^2 and scheduled maintenance of every five years with a cost of 2 $/m^2 are assumed for EIFS panel. The maintenance costs of other nonstructural components (e.g., roof), HVAC system, electrical facilities, and etc. are also considered in the LCC analysis according to the office building prototype in the Whitestone M&R data [21].

4.1.3. Annual energy cost

A cost of carbon emission, i.e., the equivalent CO_2 emission cost, is added to the building energy cost based on the amount of energy use and the source energy makeup. The Mid-case projected equivalent CO_2 unit price in tone of Synapse Energy Economics [40] is used to calculate the life-cycle carbon cost.

Fig. 7 compares the annual energy cost and source energy makeup of the archetype spatial frame (SF) buildings with various cladding options in Los Angeles, Memphis, and Boston. The city-based electricity source energy makeup is used to calculate the equivalent CO_2 footprint, where Memphis has the highest equivalent CO_2 due to the high percentage of energy from coal-fire power plants. Building archetypes in Boston consume the highest energy for indoor heating due to its cold winter. Note that since gas-heating is assumed, the heating energy costs are lower than that of cooling energy. EIFS and PCC envelope systems have similar energy performance, which are generally better than GCW across all three studied regions. This is consistent with previous studies by Aksamija and Peters [41] that opaque envelopes typically have more mass, greater insulation levels, and better heat retention than glazed envelopes, which result in less energy consumption.

For archetype buildings with GCW cladding, the glazing type has a significant impact on the annual energy consumption. GCW cladding with high-performance glazing – i.e., triple-glazed low-E glass (TriLE), vacuum glazing (VacG), and thermochromic glazing (TCG), consume 24–36% less heating and cooling energy than the baseline with double-pane glass (DPG). Across all three studied regions, vacuum glazing (VacG) shows the highest energy-saving potential. It is also noticed that since the energy performance of thermochromic glasses (TCG) is a function of temperature, it brings more energy saving potential for

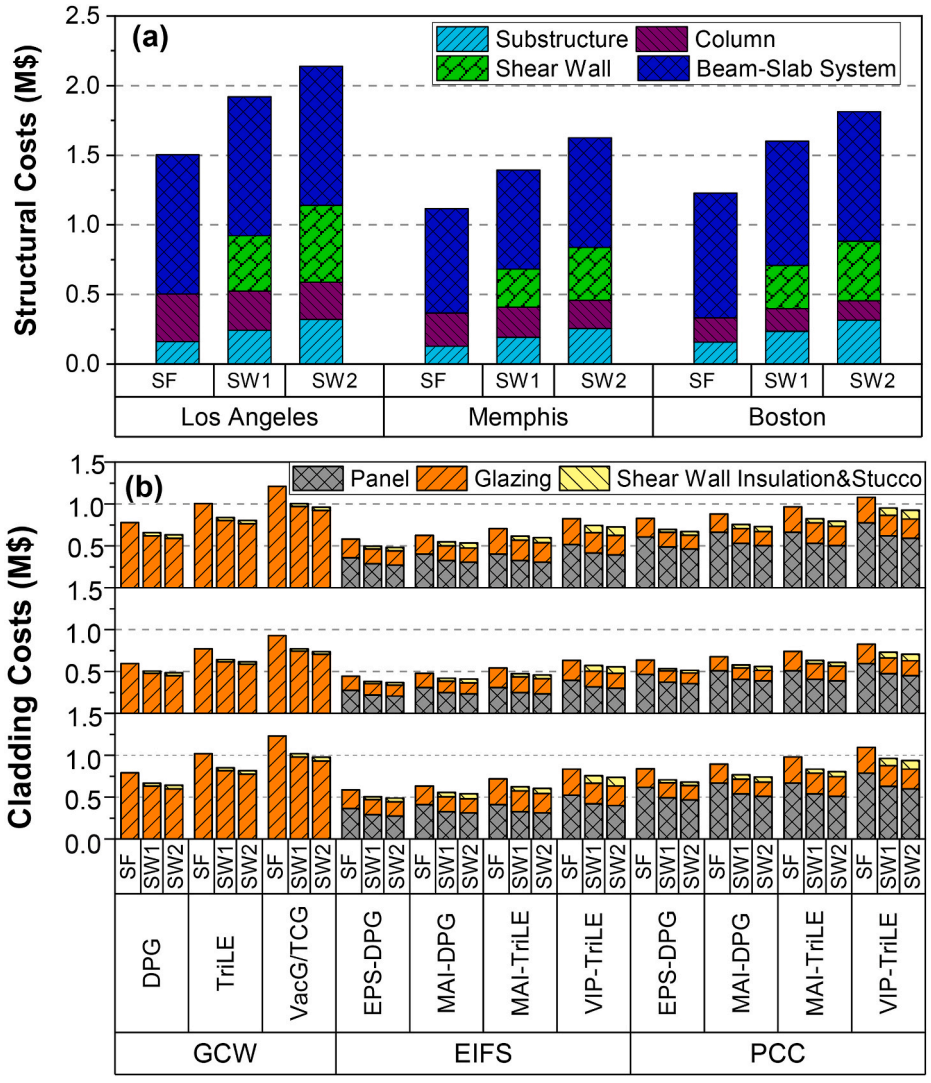

Fig. 6. Construction costs of (a) structural systems and (b) claddings in Los Angeles, Memphis, and Boston.

buildings situated in hot climate zones [42]. The study of Lee et al. [43] also indicated that TCG has similar energy performance as low-E glass. Such a result is also obtained in the current study, where the energy consumption of the building with triple-pane TCG is comparable to building with triple-pane low-E glass. For buildings with EIFS cladding, the adoption of high-performance vacuum insulation panels, such as the MAI, offer relatively limited energy-saving, where only 4%–6% of heating and cooling energy-saving was observed as compared to the ASHREA complied R-13 insulation baseline). This is due to the fact that the energy-saving potential brought by increasing the envelope's insulation (R-value) becomes limited when R-value exceeds a certain value [44]. The cost effectiveness of increasing building envelope's insulation will be discussed in the following section.

4.1.4. Seismic monetary loss

The damage and loss analysis due to seismic hazard are evaluated using FEMA P-58 PACT [6], which provides a database of repair cost/-time and other consequence functions for performing component-level loss estimation. The fragility functions obtained from the nonlinear dynamic analysis (see Section 3.3) are used to find the probability of a damageable component reaching a certain damage state.

Fig. 8 presents the expected seismic monetary losses at each hazard level and the component-level annual expected seismic monetary losses of the archetype building located in Los Angeles, CA. The expected seismic loss at each hazard level is calculated as the summation of the expected non-collapse building repair costs and the total building replacement cost considering its collapse probability at each hazard level. Fig. 8 (a), (b), and (c) show the expected seismic monetary losses at six different ground shaking hazard levels (HLs), with the return periods of 50 years (S_a (T = 0.5s) = 0.3 g (HL 1)), 100 years (S_a = 0.5 g (HL 2)), 500 years (S_a = 1 g (HL 3)), 1000 years (S_a = 1.3 g (HL 4)), 2000 years (S_a = 1.6 g (HL 5)), and 5000 years (S_a = 2.2 g (HL 6)), for archetype buildings with GWC, EIFS, and PCC, respectively. It is clear from the results that the seismic enhanced designs, i.e., SW1 and SW2, greatly reduced the expected seismic monetary loss for each hazard level. The component-level annual expected seismic monetary loss of Los Angeles archetype buildings with different cladding options are presented in Fig. 8 (d). Architype buildings with PCC cladding has higher seismic loss than those with other cladding types, mainly due to the additional weight of the cladding system which increased the lateral displacement level during a seismic event. The damage loss can be greatly reduced by adding shear walls. As expected, seismic loss increases as the more expensive energy-saving features (e.g., high-performance glazing and insulation) are used, whereas the difference is minimum for seismic enhanced buildings (i.e., SW1 and SW2). This indicates that hazard enhancement designs are effective in protecting the high-performance envelope options. Since Memphis and Boston have much lower seismic activities than that of Los Angeles, the

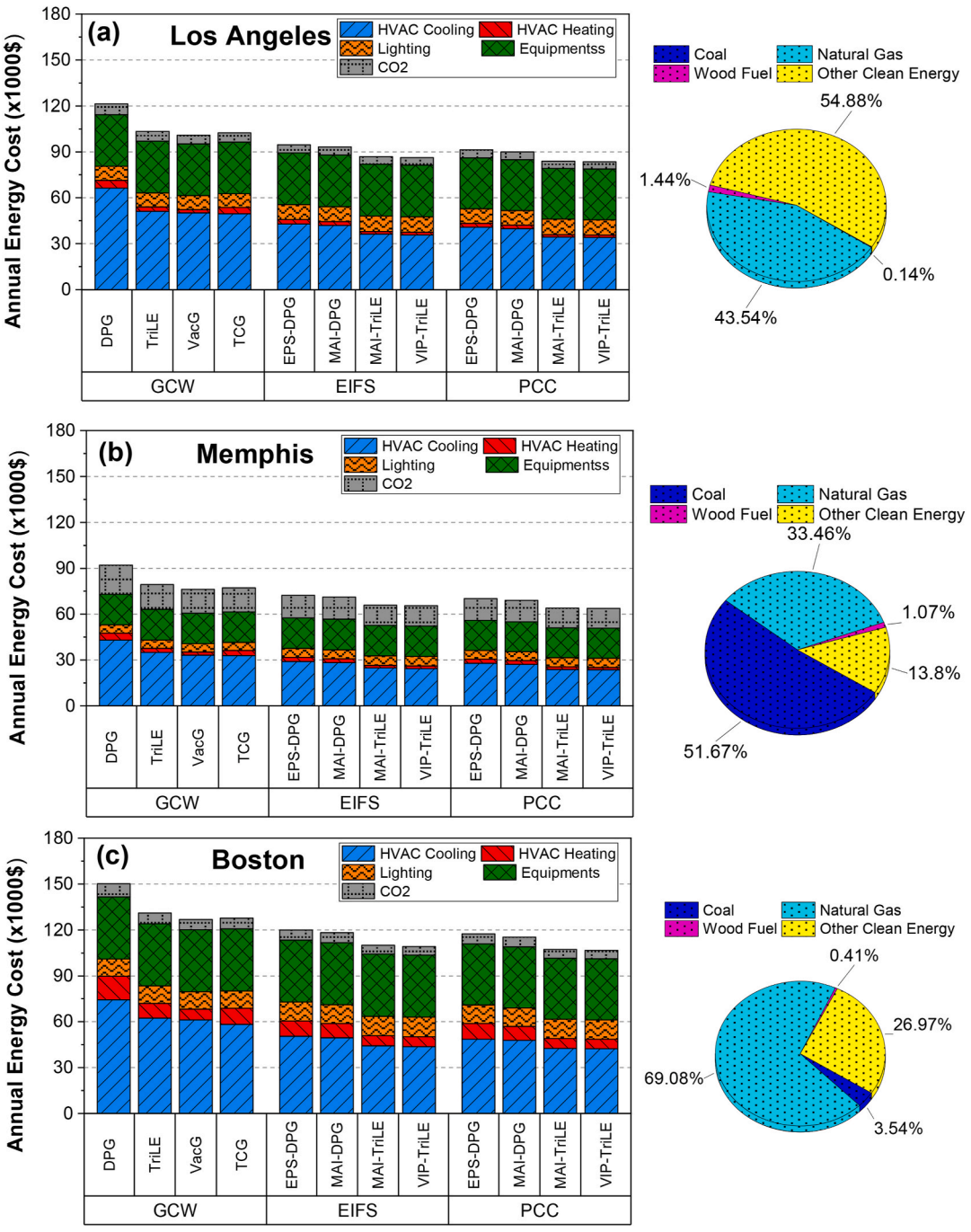

Fig. 7. Annual energy cost and electricity source energy makeup of archetype spacial frame (SF) buildings with various envelope situated in: (a) Los Angeles; (b) Memphis; and (c) Boston.

expected damage loss to due earthquake hazard is relatively small. Thus, the benefits of seismic enhanced design are limited – i.e., in these regions, spatial frame buildings are more desired due to its lower construction cost and better flexibility for architectural features and mechanical, electrical and plumbing (MEP) installations.

4.1.5. Life-cycle cost (LCC)

The 50-year LCC of the archetype office buildings with no glazing material replacement (i.e., glazing material service life longer than 50 years) located in Los Angeles (CA), Memphis (TN) and Boston (MA) are presented in Fig. 9 (a), (b), and (c), respectively. It is evident that in high seismic regions (e.g., Los Angeles, CA), seismic enhancement designs (i.e., SW1 and SW2) greatly reduce the buildings 50-year life cycle cost (LCC), see Fig. 9 (a). For the archetype building in Memphis, TN, the LCC across different structural configurations are very close, since the increased construction cost for the seismic enhanced options (i.e., shear walls) almost equals to the life-cycle seismic monetary loss savings brought by the seismic enhancement design. It is also noted that the LCC of Memphis archetype buildings are lower than buildings in Los Angeles and Boston, mainly owing to the lower construction and maintenance cost and lower energy price (as adjusted by the city-based cost index, see Table 6). For buildings located in low-seismic and cold-climate zone such as Boston, MA, the spatial frame (SF) structures are more desirable due to their relatively low construction costs.

For buildings across all geographic locations studied, EIFS cladding shows the greatest cost benefit owning to its lower construction cost,

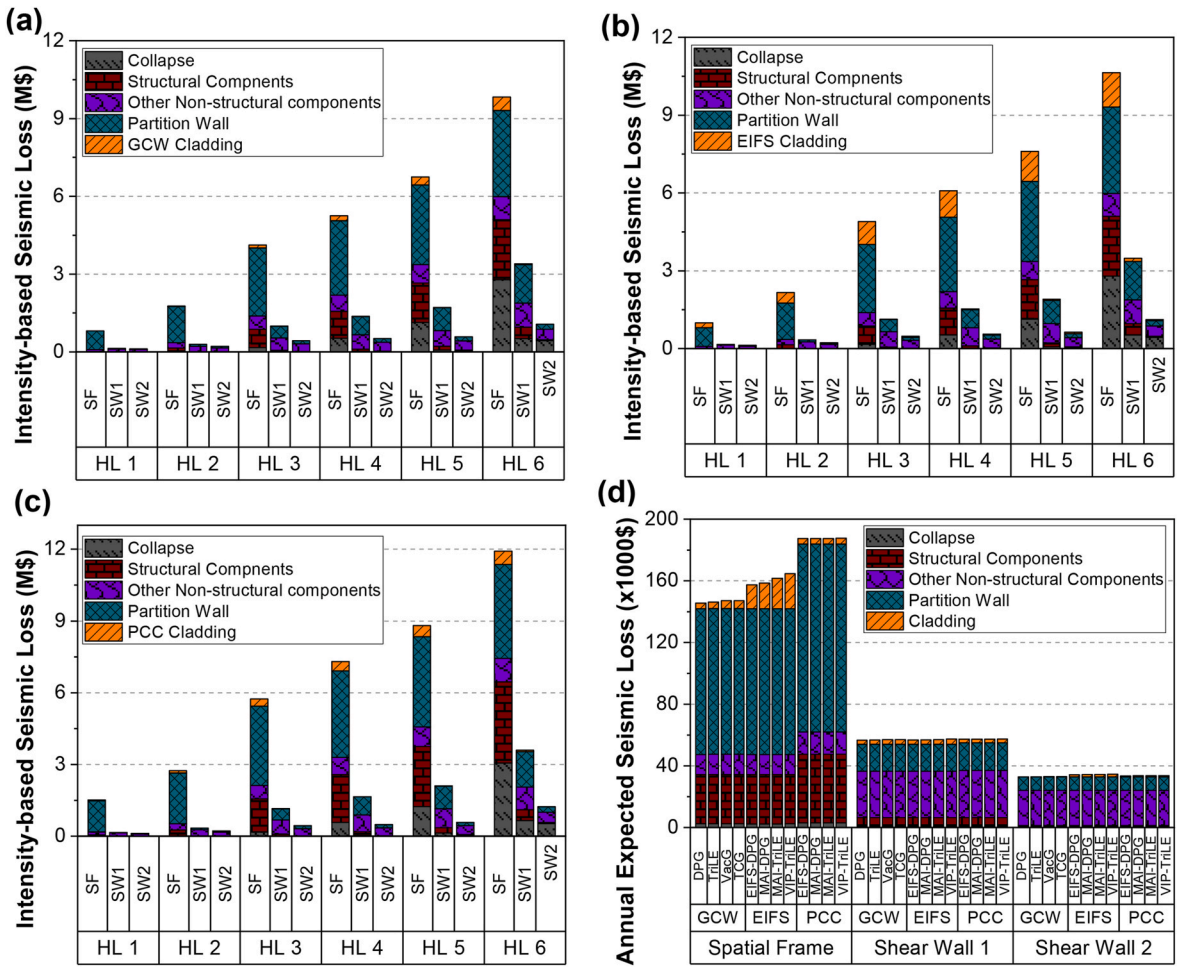

Fig. 8. Seismic monetary loss of Los Angeles archetype buildings: (a), (b), and (c) intensity-based seismic loss of Los Angeles archetype buildings with GCW, EIFS, and PCC claddings at different hazard levels; and (d) annual expected seismic loss of archtype building in Los Angeles, CA.

good energy performance, and relatively lower maintenance costs as compared to glass curtain walls. However, because of its lower stiffness, both the EIFS cladding panels and the windows are prone to damage during earthquake events. In addition, EIFS may be more prone to moisture damage in regions with hot and humid climate [45]. It is also noted that spatial frame buildings with precast concrete claddings (PCCs) are less desirable in high seismic regions due to its high self-weight acting on the building structure, see Fig. 8 (d). With seismic enhanced designs, the LCC differences between different envelope types become much smaller – if more expensive envelope options such as glass curtain wall are desired in high seismic regions, adding hazard enhancement design would greatly help to protect the asset and reduce the overall LCC of buildings. It was also observed that for low seismic regions, particularly areas with lower construction cost index (such as Memphis), PCC makes an excellent envelope option owing to its excellent durability (low maintenance cost) and good energy performance (due to its high thermal mass).

Fig. 10 presents the LCC sensitivity of archetype buildings with different structural configurations and EIFS-DPG cladding. The annual seismic loss distributions (Fig. 10 (a)) indicate that the seismic enhanced options can effectively reduce the seismic loss for buildings situated in a high seismic risk region such as Los Angeles. The annual seismic loss has a lognormal distribution and the cumulative distribution function represents the uncertainty caused by ground motions, component fragility functions and their associated repair costs. The influence of the uncertainty of the annual seismic loss on the estimated life cycle cost (LCC) is shown in Fig. 10 (b) – the LCCs of archetype buildings with different structural configurations are consistence with each other for annual seismic losses at 25 percentile, median (50 percentile), and 75 percentile.

4.2. Payback analysis for energy saving envelope designs

The payback curve as illustrated in Fig. 11 (a) is calculated as the difference in LCC between the energy-saving design and the ASHREA 90.1 complied baseline, plotted as a function of time, *T*. The solid and dashed and short dashed dot lines in Fig. 11 (a) represent the net present value of the cumulative future cost difference between the energy-saving envelope design and that of the baseline with and without considering the earthquake-induced repair and replacement cost of the structural and nonstructural components in the LCC calculation. The difference of LCC with and without considering seismic damage costs are notable in high-seismic regions such as Los Angeles – i.e., the investment into energy-efficient envelope designs takes longer to payback with the consideration of seismic damage due to the extra seismic repair costs; whereas this difference are minimum (if any) for medium- or low-seismic regions, see Fig. 12. The dashed line and short dashed dot represent the 50 years service life of glazing material (no replacement is needed in the 50 years LCC) while short dashed dot consider 30 years service life of glazing material (replacement is required at 30 years service life) respectively. It is clear that the consideration of glazing material replacement at 30 years may lead to a longer discounted payback period (DPP).

For buildings located in high-seismic regions, adding seismic

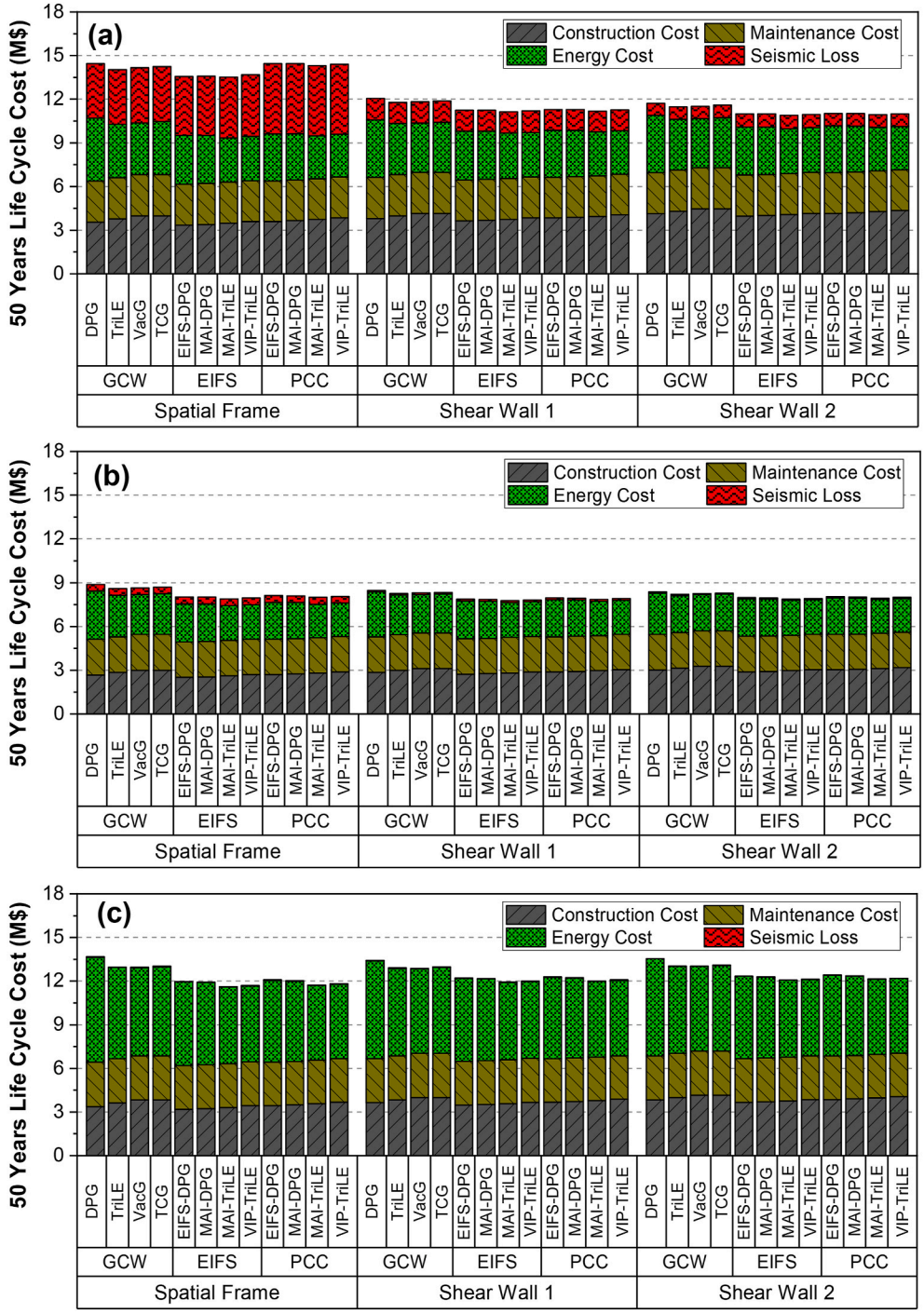

Fig. 9. 50-year life-cycle cost (LCC) of various archetype buildings located in: (a) Los Angeles, (b) Memphis, and (c) Boston.

enhancement measures, such as shear wall, greatly reduces the DPP of the more expensive glazing and insulations in EIFS system by reducing the seismic loss of the building envelope, see Fig. 11 (b). Whereas shear walls have shown little effect on the DPP of the high-performance glazing in glass curtain walls. This is because the enhanced seismic design of GCW advanced by recent recommendation for practical building installation [24] greatly increased the earthquake performance of GCW system - the glass-to-frame clearance helps to reduce clashing between glass and the frame. The shear wall designs show most benefit with EIFS cladding as the shear walls, to a large extend, reduce the interstory drift, which help to reduce the damage of windows and fenestrations in the EIFS system. Due to the high stiffness of certain types of PCC panels, the window damage in PCC largely reduced, therefore, the benefit of shear wall design is not as evident.

Fig. 12 (a), (b), and (c) compare the discounted payback period (DPP) (3% discount rate) of different glazing and insulation options for GCW, EIFS, and PCC, respectively. It is observed that high-performance glazing has a relatively shorter DPP as compared to high R-value insulations when compared to the ASHREA 90.1 complied baseline. With respect to different geographic locations, the DPP of energy-saving options for archetype buildings located in cold regions such as Boston are much shorter than that in Los Angeles and Memphis. The consideration of glazing materials replacement at 30 years service life generally increases the DPP with high-performance glazing materials. For archetype

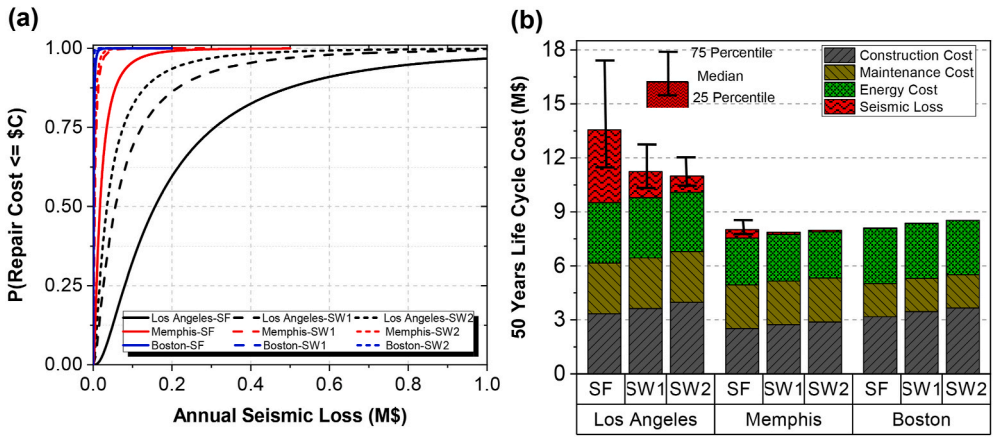

Fig. 10. LCC sensitivity of building archetypes with different structural configurations and EIFS-DPG envelope: (a) annual seismic loss distributions; (b) sensitivity of LCC to annual seismic loss.

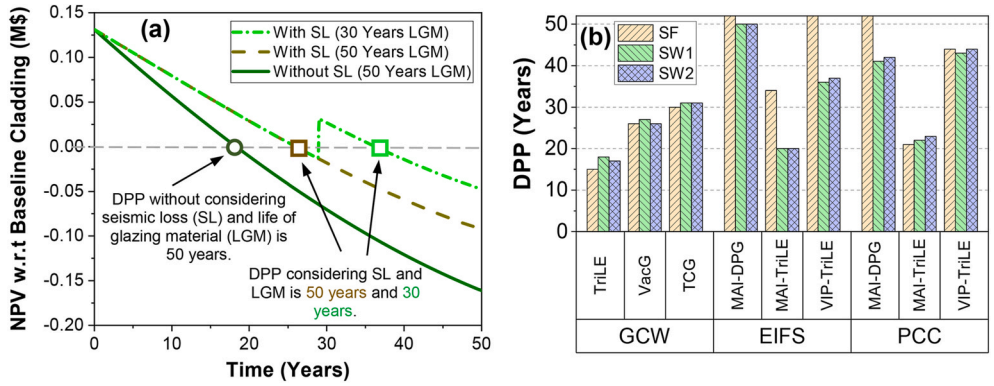

Fig. 11. (a) Discounted payback periods (DPP) of cladding with and without considering earthquake-induced seismic loss and glazing material replacement at 30 years service life; and (b) effect of seismic enhanced options for DPP (0.03 discount rate) of buidlings situated in Los Angeles without glazing material replacement.

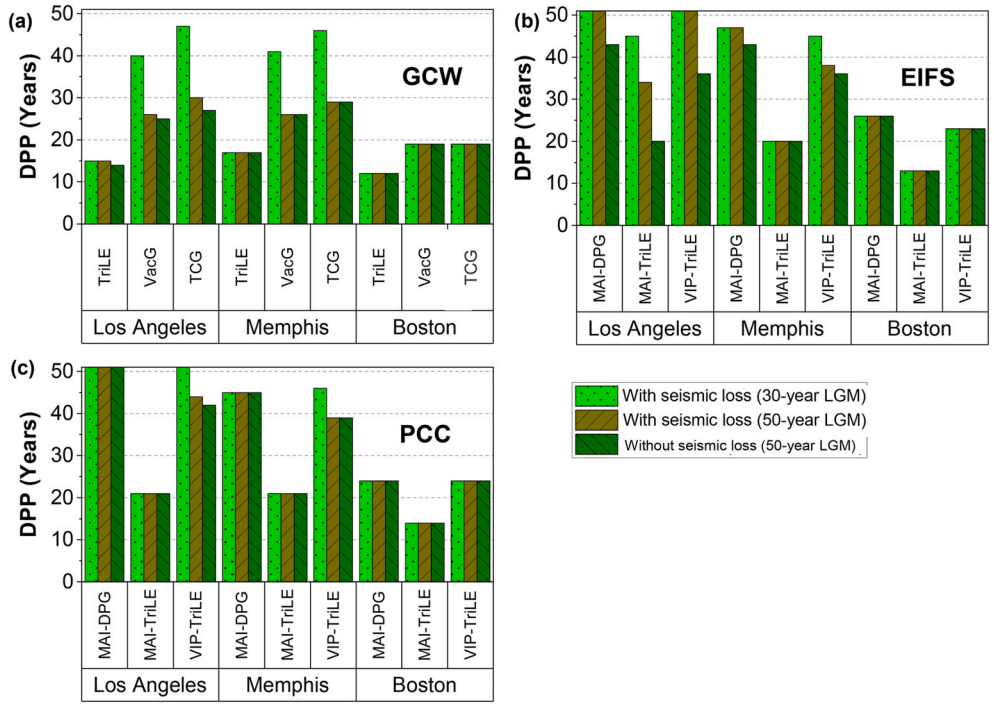

Fig. 12. Discounted payback periods (DPP) (0.03 discount rate) of spatial frame buildings with claddings of: (a) GCW, (b) EIFS, and (c) PCC situated in Los Angeles, Memphis, and Boston.

buildings located in Boston, the DPP is not impacted much by this assumption since the high performance glazings are generally paid back within 20–25 years.

In addition, the DPP is influenced by the discount rates assumed. Higher discount rates tend to favor alternatives with lower construction costs, shorter service life and higher maintenance cost and lower discount rates have reversed effects [46]. Fig. 13 presents the effects of discount rates to the discounted payback periods (DPP) of LA-SW2 archetype buildings with different cladding types. As expected, the DPP increases with the increasing of discount rates since they have higher construction costs as compared with their corresponding baseline cases.

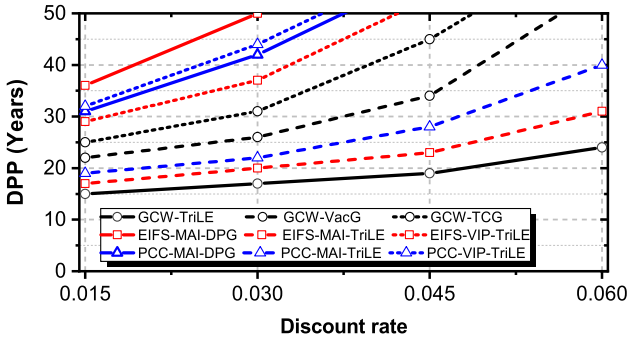

Fig. 13. Sensitivity of discounted payback periods (DPP) to discount rate (0.015–0.06) for LA-SW2 arechetype buildings with (a) GCW; (b) EIFS; and (c) PCC.

5. Concluding remarks

This research proposed a co-design framework for building structures and envelope systems, holistically considering the buildings' life-cycle cost (LCC) as impacted by its energy efficiency and structural performance when subjected to natural hazards (i.e., earthquakes). The proposed method is a two-stage LCC-informed building design process, aiming to satisfy various design requirements and provide a quantitative guideline for building structural design and envelope selection based on the geographic location of the building. The LCC analysis method accounts for the long-term energy performance of buildings, as well as expected costs associated with the repair and replacement costs due to seismic damaged. Discounted payback period analysis was conducted to assess the long-term cost-effectiveness of energy-efficient building envelope options such as high performance glazings and high R-value insulations. The method was demonstrated through the case study of medium-size office building archetypes situated in geographic locations with distinct climate conditions and seismic activities – i.e., Los Angeles, CA, Memphis, TN, and Boston, MA. Different structural configurations, including spatial frame and two seismically enhanced shear wall structures were considered. Three envelope types – i.e., glass curtain wall (GCW), exterior insulation and finish system (EIFS), and precast concrete cladding (PCC), along with different glazing and insulation types, were studied as design alternatives. The results indicated that:

- In high seismic regions, such as Los Angeles, seismic enhanced structural system design shows notable benefit since it leads to lower seismic loss despite its higher initial construction cost. The higher initial construction of seismic enhanced structural design will be quickly paid back. Particularly for building envelopes that are prone to seismic damage (i.e., EIFS), shear walls greatly reduced the interstory drift during an earthquake, protecting the fenestration and cladding panels from damage. If more expensive envelope options such as high performance glazings are desired in high seismic regions, adding hazard enhancement design (e.g., shear wall, building dampers) would greatly help to protect the asset and reduce the PDD.
- EIFS cladding shows the greatest cost benefit owning to its lower construction cost, good energy performance, and relatively lower maintenance cost. However, when used in high seismic regions both the EIFS cladding panels and the windows are prone to seismic damage because of its lower stiffness. PCC shows good cost-effectiveness in medium and low seismic regions due to its low maintenance cost and good energy performance (high thermal mass).
- More comprehensive cost benefit analysis is desired for future studies. For example, this study does not consider other ancillary benefits of adopting energy-saving options such as peak electricity reduction, space saving [39], living comfort, protection against external noise, improved indoor air quality, improved leasing potential [47]. Moreover, marginal cost and benefit of energy efficiency analysis may be needed to quantify the marginal cost and benefit of adopting different energy-saving options. This is because the energy saving potential for high-performance options is not linear related to the increased material cost, e.g., the R-value of insulation material exceeding certain value leads to negligible energy cost saving due to the so-called the law of diminishing returns [48].

CRediT authorship contribution statement

Zhenglai Shen: Methodology, Software, Investigation, Writing - original draft. **Hongyu Zhou:** Project administration, Conceptualization, Funding acquisition, Writing - review & editing. **Som Shrestha:** Writing - review & editing.

Declaration of competing interest

The authors declare that they have no known competing financial interests or personal relationships that could have appeared to influence the work reported in this paper.

Acknowledgements

This research was in part supported by the US National Science Foundation (CMMI-1954517, DEG-1623657) and the U. S. Department of Energy Office of Energy Efficiency and Renewable Energy, Building Technologies Office.

References

[1] International Energy Agency, Energy Efficiency Indicators: Essentials for Policy Making, 2014.
[2] M.S. Kappes, M. Keiler, K. von Elverfeldt, T. Glade, Challenges of analyzing multi-hazard risk: a review, Nat. Hazards 64 (2012) 1925–1958, https://doi.org/10.1007/s11069-012-0294-2.
[3] R. Ruparathna, K. Hewage, R. Sadiq, Improving the energy efficiency of the existing building stock: a critical review of commercial and institutional buildings, Renew. Sustain. Energy Rev. 53 (2016) 1032–1045, https://doi.org/10.1016/j.rser.2015.09.084.
[4] S.B. Sadineni, S. Madala, R.F. Boehm, Passive building energy savings: a review of building envelope components, Renew. Sustain. Energy Rev. 15 (2011) 3617–3631, https://doi.org/10.1016/j.rser.2011.07.014.
[5] T. Mcallister, NIST technical note 1795: developing guidelines and standards for disaster resielince of the built environment: a research needs assessment. https://doi.org/10.6028/NIST.TN.1795, 2013.
[6] Federal Emergency Management Agency, FEMA P-58: Seismic Performance Assessement of Buildings. Washington, DC, 2012.
[7] G. Mosqueda, K.A. Porter, J. O'Connor, P. McAnany, Damage to engineered buildings and bridges in the wake of hurricane Katrina, in: Forensic Eng. Symp, American Society of Civil Engineers, Long Beach, CA, 2007, https://doi.org/10.1061/40943(250)4.
[8] A. Baird, S. Pampanin, Façade damage assessment of concrete buildings in the 2011 Christchurch earthquake, Struct. Concr. 13 (2012) 3–13, https://doi.org/10.1002/suco.201100040.
[9] J. Kneifel, Life-cycle carbon and cost analysis of energy efficiency measures in new commercial buildings, Energy Build. 42 (2010) 333–340, https://doi.org/10.1016/j.enbuild.2009.09.011.
[10] T.M.I. Mahlia, A. Iqbal, Cost benefits analysis and emission reductions of optimum thickness and air gaps for selected insulation materials for building walls in

Maldives, Energy 35 (2010) 2242–2250, https://doi.org/10.1016/j.energy.2010.02.011.
[11] J. Morrissey, R.E. Horne, Life cycle cost implications of energy efficiency measures in new residential buildings, Energy Build. 43 (2011) 915–924, https://doi.org/10.1016/j.enbuild.2010.12.013.
[12] K. Perini, P. Rosasco, Cost-benefit analysis for green façades and living wall systems, Build. Environ. 70 (2013) 110–121, https://doi.org/10.1016/j.buildenv.2013.08.012.
[13] M (Max) Liu, B. Mi, Life cycle cost analysis of energy-efficient buildings subjected to earthquakes, Energy Build. 154 (2017) 581–589, https://doi.org/10.1016/j.enbuild.2017.08.056.
[14] S.J. Welsh-Huggins, A.B. Liel, Evaluating multiobjective outcomes for hazard resilience and sustainability from enhanced building seismic design decisions, J. Struct. Eng. 144 (2018), 04018108, https://doi.org/10.1061/(ASCE)ST.1943-541X.0002001.
[15] A. Noshadravan, T.R. Miller, J.G. Gregory, A lifecycle cost analysis of residential buildings including natural hazard risk, J. Construct. Eng. Manag. 1–10 (2017), https://doi.org/10.1061/(ASCE)CO.1943-7862.0001286.
[16] C. Ji, T. Hong, H.S. Park, Comparative analysis of decision-making methods for integrating cost and CO2 emission – focus on building structural design, Energy Build. 72 (2014) 186–194, https://doi.org/10.1016/j.enbuild.2013.12.045.
[17] Z.S.M. Nadoushani, A. Akbarnezhad, Effects of structural system on the life cycle carbon footprint of buildings, Energy Build. 102 (2015) 337–346, https://doi.org/10.1016/j.enbuild.2015.05.044.
[18] A. Belleri, A. Marini, Does seismic risk affect the environmental impact of existing buildings? Energy Build. 110 (2016) 149–158, https://doi.org/10.1016/j.enbuild.2015.10.048.
[19] NIST, Energy Price Indices and Discount Factors for Life-Cycle Cost Analysis – 2018, 2018.
[20] RSMeans. RSMeans, Data Online, Gordian, Rockland, MA, 2018.
[21] Whitestone Research, The Whitestone facility maintenance and repair cost reference 2009-2010. www.whitestoneresearch.com, 2009.
[22] S. Günay, K.M. Mosalam, PEER performance-based earthquake engineering methodology, revisited, J. Earthq. Eng. 17 (2013) 829–858, https://doi.org/10.1080/13632469.2013.787377.
[23] J.W. Baker, An Introduction to Probabilistic Seismic Hazard Analysis (PSHA), Stanford University, San Joe, 2008.
[24] W.C.O. Brien, A.M. Memari, M. Eeri, P.A. Kremer, R.A. Behr, M. Eeri, Fragility Curves for Architectural Glass in Stick-Built Glazing Systems 2 (2012) 639–665, https://doi.org/10.1193/1.4000011.
[25] K. Biswas, A. Desjarlais, D. Smith, J. Letts, J. Yao, T. Jiang, Development and thermal performance verification of composite insulation boards containing foam-encapsulated vacuum insulation panels, Appl. Energy 228 (2018) 1159–1172, https://doi.org/10.1016/j.apenergy.2018.06.136.
[26] J.P. Hunt, Performance Assessment and Probabilistic Repair Cost Analysis of Precast Concrete Cladding Systems for Multistory Buildings, University of California, Berkeley, 2010, https://doi.org/10.1016/j.physbeh.2008.04.026.
[27] R.A. Behr, A. Belarbi, A.T. Brown, Seismic preformance of architectural glass in a storefront wall system, Earthq. Spectra 11 (1995) 367–391.
[28] A.C. Baird, Seismic Performance of Precast Concrete Cladding Systems by, University of Canterbury, 2014, https://doi.org/10.1108/03090561011032315.
[29] K. McMullin, Y. Wong, C. Choi, K. Chan, Seismic performance states of precast concrete cladding connections, in: Proc. 13th World Conf. Earthq. Eng., Vancouver, Canada, 2004.
[30] M. AlHamaydeh, N. Aly, K. Galal, Impact of seismicity on performance and cost of RC shear wall buildings in dubai, United Arab Emirates, J. Perform. Constr. Facil. 31 (2017), 04017083, https://doi.org/10.1061/(ASCE)CF.1943-5509.0001079.
[31] E. Asadi, Z. Shen, H. Zhou, A. Salman, Y. Li, Risk-informed multi-criteria decision framework for resilience , sustainability and energy analysis of reinforced concrete buildings, J. Build. Perform. Simul. (2020), https://doi.org/10.1080/19401493.2020.1824016.
[32] ASHRAE 90.1, Energy Standard for Buildings except Low-Rise Residential Buildings, 2016.
[33] C. Christensen, R. Anderson, S. Horowitz, A. Courtney, J. Spencer, BEopt™ Software for Building Energy Optimization: Features and Capabilities, National Renewable Energy Laboratory, 2006.
[34] E. Cuce, S.B. Riffat, A state-of-the-art review on innovative glazing technologies, Renew. Sustain. Energy Rev. 41 (2015) 695–714, https://doi.org/10.1016/j.rser.2014.08.084.
[35] M. Deru, K. Field, D. Studer, K. Benne, B. Griffith, P. Torcellini, et al., U.S. Department of Energy commercial reference building models of the national building stock. Publ 1–118 (2011) https://doi.org/NREL_Report_No_TP-5500-46861.
[36] J. Zhang, G. Liu, Energy Savings for Occupancy-Based Control (OBC) of Variable-Air-Volume (VAV) Systems, Pacific Northwest National Laboratory, 2013.
[37] K. Kolozvari, K. Orakcal, J.W. Wallace, Modeling of cyclic shear-flexure interaction in reinforced concrete structural walls. I: theory, J. Struct. Eng. 141 (2015), 04014135, https://doi.org/10.1061/(ASCE)ST.1943-541X.0001059.
[38] FEMA P695, Quantification of building seismic performance factors. Washington DC, US. https://doi.org/10.1016/j.compstruc.2009.08.001, 2009.
[39] M. Alam, H. Singh, S. Suresh, D.A.G. Redpath, Energy and economic analysis of Vacuum Insulation Panels (VIPs) used in non-domestic buildings, Appl. Energy 188 (2017) 1–8, https://doi.org/10.1016/j.apenergy.2016.11.115.
[40] P. Luckow, E.A. Stanton, S. Fields, B. Biewald, S. Jackson, J. Fisher, et al., Carbon dioxide price forecast. Cambridge, MA: 2015, 2015 https://doi.org/617.661.3248.
[41] A. Aksamija, T. Peters, Heat transfer in facade systems and energy use: comparative study of different exterior wall types, J. Architect. Eng. 23 (2017) 1–17, https://doi.org/10.1061/(ASCE)AE.1943-5568.0000224.
[42] M. Saeli, C. Piccirillo, I.P. Parkin, R. Binions, I. Ridley, Energy modelling studies of thermochromic glazing, Energy Build. 42 (2010) 1666–1673, https://doi.org/10.1016/j.enbuild.2010.04.010.
[43] E.S. Lee, L.L. Fernandes, C.H. Goudey, C.J. Jonsson, D.C. Curcija, X. Pang, et al., A pilot demonstration of electrochromic and thermochromic windows in the denver federal center, Building 41 (2014).
[44] M.S. Al-Homoud, Performance characteristics and practical applications of common building thermal insulation materials, Build. Environ. 40 (2005) 353–366, https://doi.org/10.1016/j.buildenv.2004.05.013.
[45] K.C. Day, Exterior insulation finish systems: designing EIFS (clad walls) for a predictable service life, 8th Can. Conf. Build. Sci. Technol. (2001).
[46] Davis Langdon Consulting Management, Life Cycle Costing (LCC) as a Contribution to Sustainable Construction: a Common Methodology. London, Britain, 2007.
[47] M. Jakob, Marginal costs and co-benefits of energy efficiency investments the case of the Swiss residential sector, Energy Pol. 34 (2006) 172–187, https://doi.org/10.1016/j.enpol.2004.08.039.
[48] K.A. Al-sallal, Comparison between polystyrene and fiberglass roof insulation in warm and cold climates, Renew. Energy 28 (2003) 603–611.